

## Friction and wear behavior of electrodeposited amorphous Fe-Co-W alloy deposits<sup>①</sup>

HE Feng-jiao(何凤姣)<sup>1</sup>, LEI Jing-tian(雷惊天)<sup>1</sup>, LU Xin(陆欣)<sup>2</sup>, HUANG Yun-ning(黄宇宁)<sup>2</sup>

(1. College of Chemistry and Chemical Engineering, Hunan University, Changsha 410082, China;

2. Yingcai Technology Co, Ltd, High & New Technology Industry Development Region of Changsha, Changsha 410006, China)

**Abstract:** The microstructures, friction and wear behavior under dry sliding condition of electrodeposited amorphous Fe-Co-W alloy deposits heat treated at different temperatures were studied. A comparative study of hard chrome deposit under the same testing condition was also made. The experimental results show that the hardness and wear resistance of amorphous Fe-Co-W alloy deposits are improved with the increasing of heat treatment temperature, and reach the maximum value at 800 °C, then decrease above 800 °C. Under 40 N load, the wear resistance properties of the alloy deposits heat treated at 800 °C are superior to those of hard chrome deposit. The main wear mechanisms of amorphous Fe-Co-W alloy deposits heat treated below 600 °C are peeling, plastic and flowing deformation; when the deposits are heat treated above 700 °C, they are plastic and flowing deformation. While the main wear mechanisms of hard chrome are abrasive wear, fatigue and peeling.

**Key words:** electrodeposition; amorphous Fe-Co-W alloy deposits; friction and wear behavior; heat treatment

**CLC number:** TG 115.5; TG139

**Document code:** A

### 1 INTRODUCTION

Chrome electrodeposits possess attractive properties, such as high microhardness, excellent wear and corrosion resistance, decorative appearance, and have been found wide use in engineering industries. Chrome deposits are usually plated on the surface of cutting and drawing tools, bearings, measures, cylinders, and rollers and so on, to prolong their service life. They are also used to repair wearing machine parts to their primary dimension for reuse in maintenance department of automobiles, agricultural machines, and machine tools<sup>[1]</sup>. However, compared with some other deposits, the plating technique of chrome deposits has some deficiencies. Firstly, the cathode current efficiency(CCE) is very low, only 12 % - 15 % in industry production. Secondly, the throwing and covering power of the plating bath are disappointing. Special anode or protective cathode must be used to obtain uniform deposits. Thirdly, high current density (above 20 A/dm<sup>2</sup>) and high tank voltage are employed to attain qualified deposits, so the energy consumption is high. Fourthly, the electrolytic solution is strongly acidic, oxidated, corrosive and toxic. Hexavalent chrome in solution is recognized as a carcinogen<sup>[2]</sup>. For the needs of environment protection and safety and health, plating industry has been forced to seek after alternative materials which possess the same or similar appearance,

properties of chrome deposits.

Tungsten alloys exhibit high corrosion resistance and good mechanical properties. The electrodeposits of tungsten alloys are regarded as one of potential replacements of chrome deposits. Compared with chrome deposit techniques, the tungsten deposit techniques have following advantages. Firstly, the cathode current efficiency is high, which can reach 70%. Secondly, the throwing and covering power of plating bath are good. Thirdly, employing moderate current density (3 - 8 A/dm<sup>2</sup>) can obtain qualified deposits. So the energy consumption is low. Fourthly, the electrolytic solution is environmentally friendly. The electrodepositions of tungsten alloys have been studied widely. Ni-W alloy deposits obtained by electrodeposition were of high microhardness, high thermal stability and ductility, good wear and corrosion resistance<sup>[3-5]</sup>. Effect of additives on Ni-W alloys was reported<sup>[6-8]</sup>. For Co-W alloys, Svensson et al<sup>[9]</sup> studied the microstructures of alloy deposits and found that they varied from crystalline to nanocrystalline with the increasing of tungsten content in deposits. Donten<sup>[10]</sup> studied the adhesion ability of amorphous Co-W alloys to different substrates. Good adhesion to copper and poor adhesion to mild steel were found. Co-W alloys were electrodeposited from acidic bath containing cationic surfactants, and their hardness and corrosion resistance were examined and compared with those of chrome deposits<sup>[11]</sup>. Tungsten alloys

① **Foundation item:** Project(2001AA327040) supported by Hi-tech Research and Development Program of China

**Received date:** 2004 - 01 - 13; **Accepted date:** 2004 - 04 - 23

**Correspondence:** HE Feng-jiao, professor, PhD; Tel: + 86-731-8914786; E-mail: Fengjiaoh@hotmail.com

have also been deposited as barrier used for ultralarge-scale integrated and microelectromechanical system<sup>[12, 13]</sup>.

Reports about the friction and wear behavior of tungsten alloys is few<sup>[14]</sup>. In this paper, under dry sliding condition, the microstructures, friction and wear behavior of electrodeposited amorphous Fe-Co-W alloy heat treated by different temperatures were studied. A comparative study on hard chrome deposit under the same testing conditions was also made.

## 2 EXPERIMENTAL

### 2.1 Preparation of amorphous Fe-Co-W alloy deposits

Amorphous Fe-Co-W alloy deposits were plated on the surface of AISI 1045 steel. Its dimensions were  $d\ 34\text{ mm} \times 10\text{ mm}$ . The electrodeposition processes were: burnishing  $\rightarrow$  polishing  $\rightarrow$  degreasing  $\rightarrow$  rinsing  $\rightarrow$  acid activation  $\rightarrow$  rinsing  $\rightarrow$  electroplating. The electroplating bath mainly contained  $\text{FeSO}_4$ ,  $\text{CoSO}_4$ ,  $\text{Na}_2\text{WO}_4$ ,  $\text{Na}_3\text{Cit}$ ,  $\text{H}_3\text{BO}_3$  and  $\text{NH}_3 \cdot \text{H}_2\text{O}$ . The plating conditions were: pH 8.0, plating temperature  $80\text{ }^\circ\text{C}$ , cathode current density  $5.0\text{ A/dm}^2$ .

### 2.2 Heat treatment

Heat treatment were carried out in air at different temperatures in a muffle furnace. Alloy deposit samples were put in the furnace, maintained 6 min, then quenched in 8% (mass fraction, %) NaCl solution to gain higher hardness and better wear resistance.

### 2.3 Determination of component of deposits

The contents of iron, cobalt in deposits were determined with a WFX-1C atom absorption spectrophotometer. The contents of tungsten in deposits were determined with a Leng Guan 722 visual spectrophotometer.

### 2.4 Characterization

The microstructures of alloy deposits were tested by a Japan Rigaku D/max-rA X-ray diffractometer (XRD) employing Cu target,  $K_\alpha$  radiation. The temperature of phase transformation was determined by a SDT 2960 differential thermal analysis (DTA) meter.

### 2.5 Hardness

The hardness was measured with a HVS-1000 digital microhardness tester. The load was  $0.98\text{ N}$ , and the loading time was  $10\text{ s}$ . Six points on the surface of each deposit were chosen randomly to determine the hardness, and the average value was taken.

### 2.6 Friction and wear tests

The friction and wear tests were carried out with a MPX-2000 friction and wear test rig in a ring-on-disk configuration. The upper counterpart was AISI 52100 steel, whose hardness was about HV 650. Its dimensions were  $d\ 32\text{ mm}/20\text{ mm} \times 10\text{ mm}$ , and its rotative velocity was  $384\text{ r/min}$ . The lower counterpart, which was static, was deposits of about  $40\text{ }\mu\text{m}$  thick plated on AISI 1045 steel. Its dimensions were  $d\ 34\text{ mm} \times 10\text{ mm}$ . The counterparts were burnished by CC 2000 abrasive paper and degreased with absolute alcohol before wear test. The test conditions were: dry sliding, load varied from  $20\text{ N}$  to  $80\text{ N}$ . The test duration was  $60\text{ min}$ . The friction coefficient  $\mu$  was calculated through the recording data of moment. The wear resistance properties were evaluated by mass loss of unit time, or average wear rate (AWR). The mass loss of deposits after wear test was measured by a METTLER-AE 240 analysis balance with accuracy of  $0.01\text{ mg}$ . The morphologies of wear scar of deposits were observed using a KYKY-2800 scanning electron microscope (SEM).

## 3 RESULTS AND DISCUSSION

### 3.1 Effect of heat treatment temperature on microstructures of Fe-Co-W alloy deposits

The XRD patterns of Fe-Co-W alloy deposits are shown in Fig. 1. Fig. 1(a) shows that the as-deposited Fe-Co-W alloy is in amorphous phase. In Fig. 1(b), overlapped diffractive peaks of crystallized phase were observed. It means that partial crystallization appears in alloy deposits after heat treatment at  $800\text{ }^\circ\text{C}$ . The crystallized phases are  $\alpha\text{-Fe}$ . From Fig. 1(c), a lot of diffractive peaks of crystallized phase are found. It is indicated that most of amorphous phases in alloy deposits have been crystallized after heat treatment at  $900\text{ }^\circ\text{C}$ . The crystallized phases are  $\alpha\text{-Fe}$ ,  $\text{Fe}_6\text{W}_6\text{C}$ , Co (cubic system). Actually, the transformation of amorphous phase to crystalline is gradually completed during heat treatment, and undergoes a series of metastable states, does not attain stable phases directly<sup>[15]</sup>. Fig. 2 shows the differential thermal analysis (DTA) curve of Fe-Co-W alloy deposit. It can be found that there is an obvious peak at about  $805\text{ }^\circ\text{C}$ , which may be corresponding to the heat emitted from for crystallization of  $\alpha\text{-Fe}$  from amorphous phase in alloy deposits. This is consistent with the XRD results (shown in Fig. 1(b)).

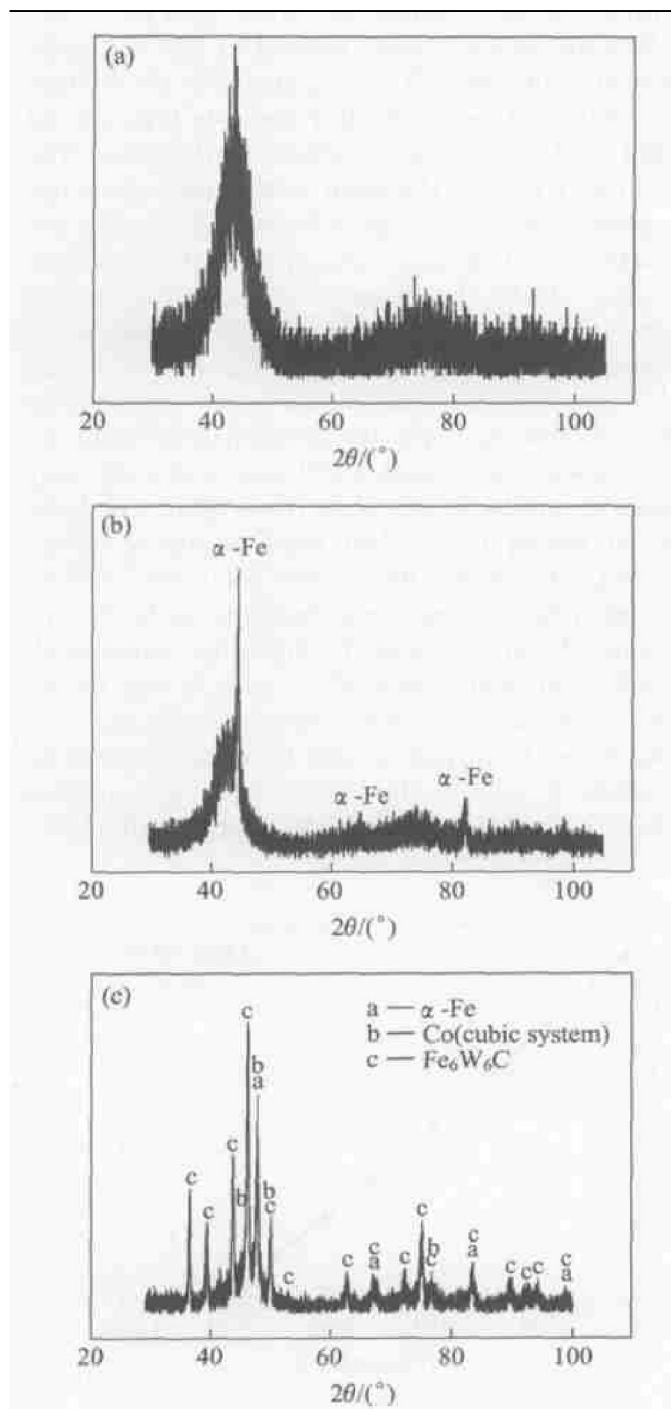


**Fig. 1** XRD patterns of Fe-Co-W alloy deposits  
(a) —as deposited;  
(b) —Heat treated at 800 °C;  
(c) —Heat treated at 900 °C

### 3.2 Effect of heat treatment temperature on hardness and friction and wear behavior of Fe-Co-W alloy deposits

#### 3.2.1 Effect of heat treatment temperature on hardness of deposits

The effect of different heat treatment temperatures on the hardness of Fe-Co-W alloy deposits is shown in Table 1. The hardness of alloy deposits increases with increasing the heat treatment temperature, and reaches the maximum value ( about 1 300 HV ) at about 800 °C . This may be caused by

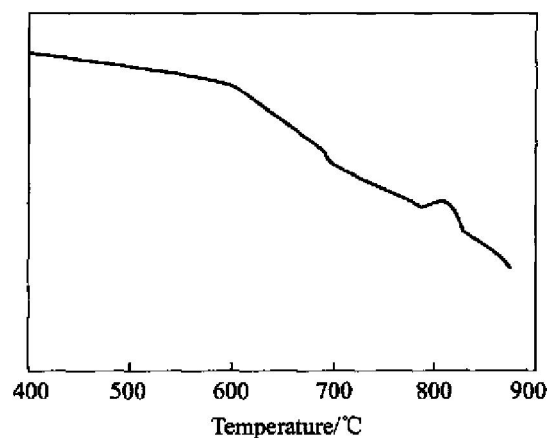


**Fig. 2** DTA curve of Fe-Co-W alloy deposits

the partial crystallization of Fe-Co-W alloy deposits and nanocrystallized  $\alpha$ -Fe phase. Then the hardness decreases above 800 °C, which may be correlated with the crystallization of most of amorphous phase in alloy deposits and the growth of crystalline grains. From Table 1, it can also be observed that the hardness of alloy deposits heat treated above 600 °C is equal to or higher than that of chrome deposit.

**Table 1** Effect of heat treatment temperature on hardness of Fe-Co-W alloy deposits

No.	Sample	Temperature/ °C	Average hardness(HV)
1 <sup>#</sup>	Fe-Co-W	As-deposited	827
2 <sup>#</sup>	Fe-Co-W	400	881
3 <sup>#</sup>	Fe-Co-W	600	985
4 <sup>#</sup>	Fe-Co-W	700	1 141
5 <sup>#</sup>	Fe-Co-W	800	1 309
6 <sup>#</sup>	Fe-Co-W	900	1 154
7 <sup>#</sup>	Cr	As-deposited	1 007

#### 3.2.2 Effect of heat treatment temperature on friction and wear behavior of deposits

Figs. 3(a), (b) show respectively the effect of heat treatment temperature on the friction coefficient  $\mu$  and average wear rate (AWR) of Fe-Co-W alloy deposits under 40 N load. It can be concluded that the friction coefficient  $\mu$  and the average wear rate (AWR) of Fe-Co-W alloy deposits vary regularly with the change of heat treatment temperature. At first they decrease with increasing the heat treatment temperature, then reach the minimum value at 800 °C, followed by increasing above 800 °C. This is also in accordance with the general law that the friction coefficient  $\mu$  is the biggest when the hardness of counterparts is close. From Fig. 3(a), it can also be found that the friction coefficient  $\mu$  of Fe-Co-W alloy deposits increases with the test duration increasing,

and reaches a steady value after 20–30 min. While the friction coefficient  $\mu$  of chrome deposit is relatively steady and higher, which is nearly equivalent to that of Fe–Co–W alloy deposit heat treated at 400 °C (No. 2<sup>#</sup>). This may be related to the change of the surface hardness of chrome deposits caused by increasing temperature of the counterparts interface during dry sliding. In fact, the hardness of hard chrome deposits begins to decrease when heat treated at 200 °C. It will decrease down to 50% primary hardness when heat treated at 600 °C, and 30% at 980 °C<sup>[16]</sup>. In this test, the average wear rate (AWR) of chrome deposit is  $3.5 \times 10^{-5}$  g/min. It can also be observed from Fig. 3(b) that under 40 N load, the average wear rate (AWR) of chrome deposit is close to those of Fe–Co–W alloy deposits heat treated at 700 °C and 900 °C ( $3.4 \times 10^{-5}$  g/min,  $3.9 \times 10^{-5}$  g/min, respectively), but bigger than that of alloy deposit heat treated at 800 °C ( $2.6 \times 10^{-5}$  g/min). This is different from the views of Capel et al<sup>[14]</sup>.

Figs. 3(c), (d) respectively show the friction coefficient  $\mu$  and average wear rate (AWR) of Fe–Co–

W alloy deposits heat treated at 800 °C under different loads. Fig. 3(c) indicates that the friction coefficient  $\mu$  of Fe–Co–W alloy deposits heat treated at 800 °C decreases with increasing the load. The reason may be that the main wear mechanisms under lower load (20 N) are plastic and flowing deformation, and the friction coefficient  $\mu$  is relatively larger. With the increase of load, the surface temperature of counterparts during the test is increased rapidly, causing the appearance of oxidation layer of high temperature, which can serve as lubricant and decrease the friction coefficient  $\mu$ . The tendency of friction coefficient  $\mu$  of each alloy deposit is similar, i. e. all increase with test duration increasing first, then reach a steady value. Fig. 3(d) shows that the average wear rate (AWR) of alloy deposits increases initially with the increasing of load, reaches the maximum value at 60 N load, then decreases at 80 N load. It may be the reason that the wear mechanisms of deposits are transformed from plastic and flowing deformation or adhesive wear under lower load to oxidation wear of high temperature under higher load.

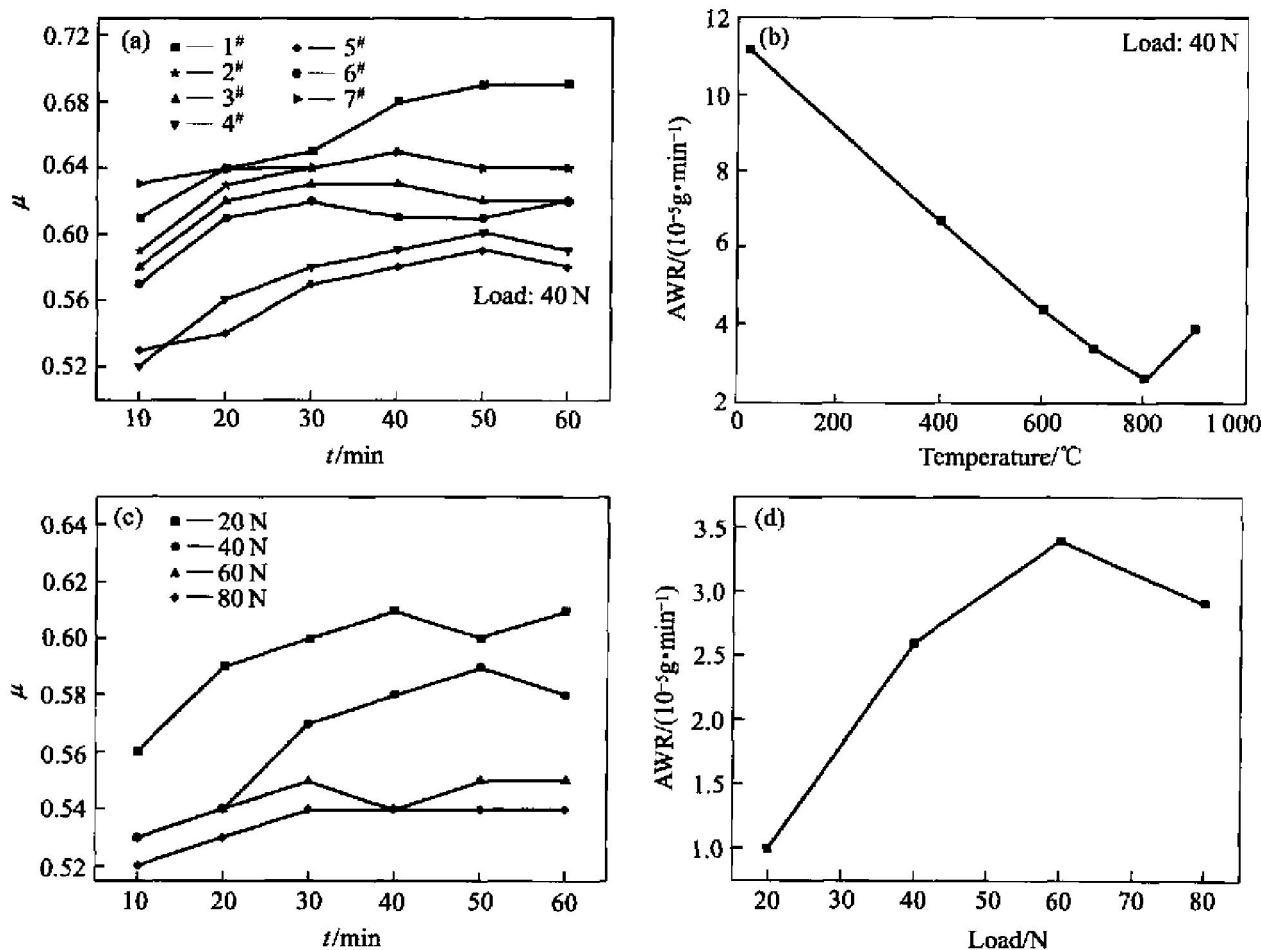


**Fig. 3** Variation of friction coefficient  $\mu$  and average wear rate (AWR) of Fe–Co–W and Cr deposits  
1<sup>#</sup> —As deposited; 2<sup>#</sup> —400 °C; 3<sup>#</sup> —600 °C; 4<sup>#</sup> —700 °C; 5<sup>#</sup> —800 °C; 6<sup>#</sup> —900 °C; 7<sup>#</sup> —Cr, as deposited

### 3.2.3 Wear mechanisms

The morphologies of wear scars of Fe-Co-W alloy deposits heat treated below 600 °C are similar to that of as-deposited alloy deposit. The wear resistance of alloy deposits is improved gradually with the increasing of heat treatment temperature. Fig. 4(a) shows the SEM morphology of wear scar of as-deposited Fe-Co-W alloy deposits under 40 N load, from which it can be found that bulk peeling and a few plastic deformations appear, and some loose structures are formed. The main wear mechanisms are peeling, plastic and flowing deformation. This may be caused by the uniformity of structure and chemical composition, and good toughness and plasticity of amorphous alloy. The morphologies of wear scars of Fe-Co-W alloy deposits heat treated above 700 °C are similar. Fig. 4(b) shows the SEM morphology of wear scar of Fe-Co-W alloy deposits heat treated at 800 °C under 40 N load. A few plastic deformations, loose structures and debris particles are found, but not bulk peeling. The main wear mechanisms are plastic and flowing deformation. This may be caused by partial crystallization of amorphous Fe-Co-W alloy deposits as

a result of heat treatment, and mixed crystalline phases improve the hardness, strength, and wear resistance of alloy deposits. Fig. 4(c) presents the representative SEM morphology of wear scar of chrome deposit under 40 N load, from which it can be found that a few thin and shallow ploughs are formed, in which some incontinuous peeling pits are dispersed. Because of the relatively high hardness of chrome deposits, hard particles are formed at the primary stage of sliding, which are pushed in the following test. The chrome deposits are cut by these particles, which bring about ploughs on the surface of deposits. The main wear mechanism is abrasive wear of hard particles. It is also observed that evident cracks and peeling debris appear, which indicates that fatigue and peeling occur. Fig. 4(d) shows the energy dispersive X-ray microanalysis(EDX) pattern of Fe-Co-W alloy deposit. The result of components in alloy deposits is in accordance with that determined by spectrophotometer, of which the contents of iron, cobalt, tungsten in deposits are respectively 50.40%, 32.69%, 16.92% (mole fraction, %).

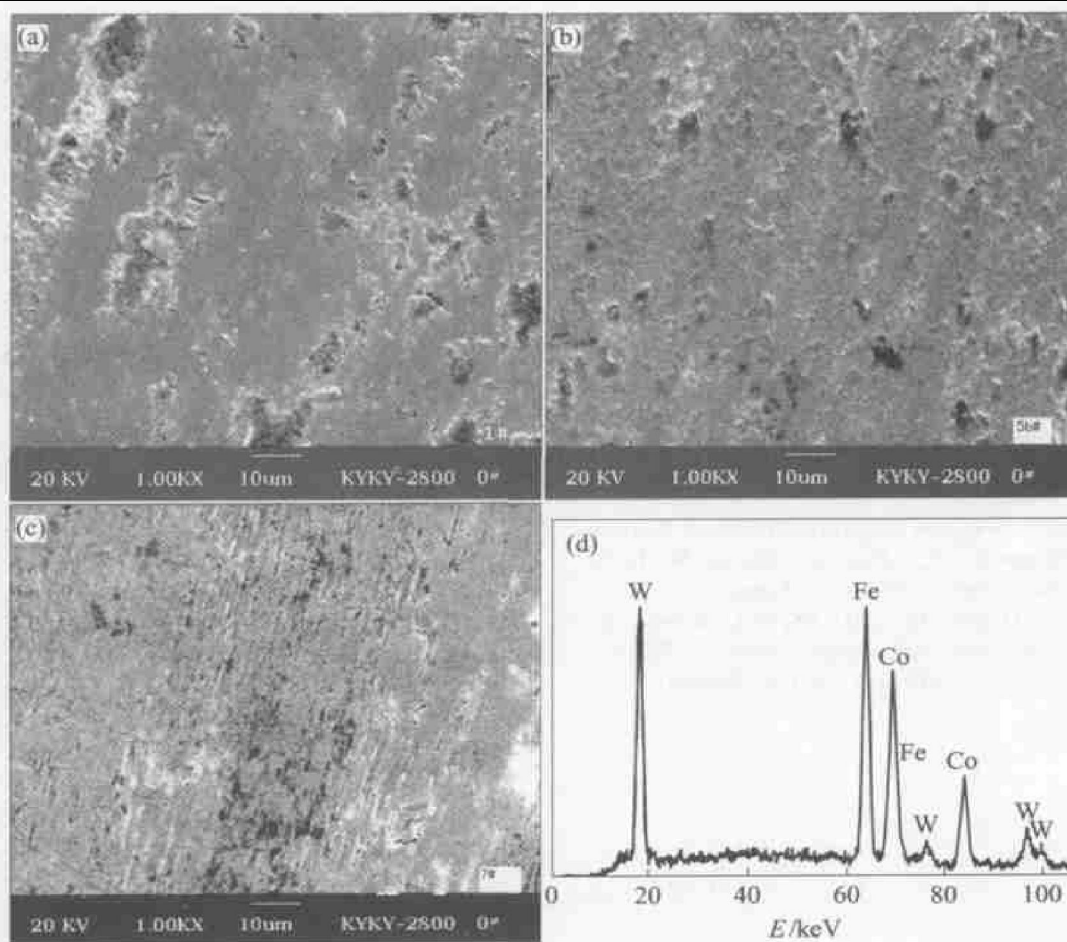


**Fig. 4** SEM morphologies and EDX pattern of wear scars of Fe-Co-W and Cr deposits under 40 N load

- (a) —As-deposited Fe-Co-W deposit; (b) —Fe-Co-W deposit heat treated at 800 °C;  
(c) —As-deposited Cr deposit; (d) —EDX pattern of wear scars of Fe-Co-W deposit



## 4 CONCLUSIONS

1) The hardness and wear resistance of amorphous Fe-Co-W alloy deposits are improved with increasing the heat treatment temperature, reach the maximum value at 800 °C, then decrease above 800 °C. Under 40 N load, the wear resistance properties of alloy deposits heat treated at 800 °C are superior to those of chrome deposit. And those of alloy deposits heat treated at 700 °C and 900 °C are equivalent to those of chrome deposit.

2) The wear rate of amorphous Fe-Co-W alloy deposits heat treated at 800 °C increases with load increasing, reaches the maximum at 60 N, then decreases at 80 N. It may be the reason that the wear mechanisms of deposits are transformed from plastic and flowing deformation or adhesive wear under lower load to oxidation wear of high temperature under higher load.

3) The wear mechanisms of amorphous Fe-Co-W alloy deposits heat treated at different temperature under 40 N load are not the same. The main wear mechanisms of alloy deposits heat treated below 600 °C are peeling, plastic and flowing deformation, and heat treated above 700 °C they are plastic and flowing deformation; while the main wear mechanisms of chrome deposit are abrasive wear, fatigue, and peeling.

## Acknowledgements

The authors would like to thank professor CHEN Xiao-hua, Material Science and Engineering College of Hunan University for supplying necessary facilities.

## REFERENCES

- [1] YAN Qir-yuan. Modern Electroplating and Surface Finishing Additives[M]. Beijing: Science & Technology Literature Press, 1994. (in Chinese)
- [2] GUAN Shan, ZHANG Qi, HU Ru-nan. Recent development of chromium electrodeposition [J]. Materials Protection, 2000, 33(3): 1-3. (in Chinese)
- [3] Stepanova L I, Purovskaya O G. Electrodeposition of Ni based alloys with tungsten and molybdenum[J]. Metal Finishing, 1998, 96 (11): 50-53.
- [4] Yamasaki T, Tomohira R, Ogino Y, et al. Formation of ductile amorphous and nanocrystalline Ni-W alloys by electrodeposition [J]. Plating & Surface Finishing, 2000, 87 (5): 148-152.
- [5] Donten M, Cesiulis H, Stojek Z. Electrodeposition and properties of Ni-W, Fe-W, Fe-Ni-W amorphous alloys. A comparative study[J]. Electrochimica Acta, 2000, 45 (20): 3389-3396.
- [6] Rodriguez. Ductility Agents for Nickel-Tungsten Alloys [P]. US 6045682. 2000-04-04.
- [7] Younes-Metzler O, Zhu L, Gileadi E. The anomalous codeposition of tungsten in the presence of nickel[J]. Electrochimica Acta, 2003, 48 (18): 2551-2562.
- [8] Wu Y Y, Chang D Y, Kim D S, et al. Effects of 2-burtyne 1, 4-diol on structures and morphologies of electroplating Ni-W alloy[J]. Surface & Coatings Technology, 2003, 162(2-3): 269-275.
- [9] Svensson M, Wahlström U, Holmbom G. Compositionally modulated cobalt-tungsten alloys deposited from a single ammoniacal electrolyte[J]. Surface & Coatings Technology, 1998, 105(3): 218-223.
- [10] Donten M, Gromulski T, Stojek Z. The interface between metallic substrates and layers of electrodeposited Co-W amorphous alloys[J]. Journal of Alloys and Compounds, 1998, 279(2): 272-278.
- [11] Abdel Hamid Z. Electrodeposition of cobalt-tungsten alloys from acidic bath containing cationic surfactants[J]. Materials Letters, 2003, 57(16-17): 2558-2564.
- [12] Shacham-Diamand Y, Lopatin S. Integrated electroless metallization for ULSI [J]. Electrochimica Acta, 1999, 44(21-22): 3639-3649.
- [13] Shacham-Diamand Y, Sverdlov Y. Electrochemically deposited thin film alloys for ULSI and MEMS applications [J]. Microelectronic Engineering, 2000, 50(1-4): 525-531.
- [14] Capel H, Shipway P H, Harris S J. Sliding wear behavior of electrodeposited cobalt-tungsten and cobalt-tungsten-iron alloys[J]. Wear, 2003, 255(20): 917-923.
- [15] Waseda Y, Okazaki H, Masumoto T. Current views on the structure and crystallization of metallic glasses[J]. Journal of Materials Science, 1977, 12(10): 1927-1949.
- [16] ZENG Hua-liang, WU Zhong-da, CHEN Jiu-wu, et al. Handbook of Electroplating Techniques[M]. Beijing: China Machine Press, 1997. (in Chinese)

(Edited by YUAN Sai-qian)